 CMES, vol.9, no.2, pp.111-131, 2005

Vibrations of Cracked Euler-Bernoulli Beams using Meshless Local Petrov-Galerkin (MLPG) Method

U. Andreaus[1,3], **R. C. Batra** [2], **M. Porfiri** [2, 3]

R. C. Batra dedicates this work to Prof. S. N. Atluri on his 60th birthday.

Abstract: Structural health monitoring techniques based on vibration data have received increasing attention in recent years. Since the measured modal characteristics and the transient motion of a beam exhibit low sensitivity to damage, numerical techniques for accurately computing vibration characteristics are needed. Here we use a Meshless Local Petrov-Galerkin (MLPG) method to analyze vibrations of a beam with multiple cracks. The trial and the test functions are constructed using the Generalized Moving Least Squares (GMLS) approximation. The smoothness of the GMLS basis functions requires the use of special techniques to account for the slope discontinuities at the crack locations. Therefore, a set of Lagrange multipliers is introduced to model the spring effects at the crack locations and relate motions of the intact beam segments. The method is applied to study static and transient deformations of a cracked beam and to determine its modal properties (frequencies and mode shapes). Numerical results obtained for a simply supported beam are compared with experimental findings, analytical predictions and finite element solutions.

keyword: MLPG method, multiple cracks, breathing crack, Lagrange multipliers, meshless method, transient analysis, modal analysis.

1 Introduction

Most load carrying systems and structures degrade or accumulate cracks during service. For safety reasons, it is desirable that any existing cracks be detected and located before they cause more serious damage and eventual system failure. Visual inspection is costly and tedious and often does not yield a quantifiable result. For some components visual inspection is virtually impossible. Therefore, the development of structural health monitoring techniques has received increasing attention in recent years (see e.g. Dimarogonas (1996)). Among these techniques, it is believed that the use of vibration data offers the most desirable alternative to actually dismantling the structure. In this method one excites the structure either in free vibration or in forced harmonic oscillations and extracts the natural frequencies and, if possible, the mode shapes. The main idea behind damage detection schemes that rely on modal data is that a damage in the system will manifest itself as changes in the modal characteristics.

The structural health monitoring and diagnostics generally require accurate models for the structures, since the measured modal characteristics generally do not change much with damage; e.g. the changes in natural frequencies due to cracks become significant only when the structure is close to failure. As for the computational costs involved in the identification procedure a good compromise between accuracy and simplicity should be a key feature of a mathematical model intended to be part of the on-line health monitoring procedure. Therefore in the last two decades, several investigators have been working on the development of reliable and robust mathematical models of damaged structural elements, especially slender beams. The different theoretical modeling techniques for cracked slender structures can be grouped in two basic categories: i) "lumped flexibility" models; and ii) "continuous" models.

The first category is based on the representation of a crack as a lumped flexibility element (generally a spring), without affecting the modeling of the undamaged regions (see e.g. Gudmunson (1983) and Chondros & Dimarogonas (1998) for modeling aspects; Ostachowicz & Krawczuk (1991) and Khiem & Lien (2004) for a multiple cracks scenario; and Rizos, Aspragathos & Di-

[1] Corresponding Author, ugo.andreaus@uniroma1.it
[2] Engineering Science and Mechanics Department, Virginia Tech, Blacksburg VA 24061, U.S.A.
[3] Dipartimento di Ingegneria Strutturale e Geotecnica, Università di Roma "La Sapienza", Via Eudossiana 18, 00184 Roma

marogonas (1988) for the damage identification). The determination of the equivalent lumped stiffness is usually performed in the framework of classical fracture mechanics, starting from the knowledge of the stress intensity factors. On the other hand, the basic idea behind the second modeling strategy is to obtain a continuous, one dimensional model of the cracked beam at the level of approximation of classical beam theory (see e.g. Christides & Barr (1984) for modeling aspects; Shen & Pierre (1990) and Shen & Pierre (1994) for computational insights; Chondros & Dimarogonas (1998) and Chondros (2001) for comparisons between the lumped flexibility and the continuous models; Carneiro & Inman (2002) for the derivation of a continuous model including shear deformations). The governing equations of the one-dimensional cracked beam are derived via a variational principle, e.g. the Hu-Washizu-Barr method. The modification of the stress field induced by the crack is incorporated through a local empirical function which assumes an exponential decay with the distance from the crack. This additional crack function can be determined in several ways, but none of them seems to be satisfactory. The adopted techniques range from crude numerical analysis to experimental investigations passing through qualitative fracture mechanics. For a complicated structure with multiple cracks, the solution of the governing equations of motion requires numerical techniques, e.g. the finite element method (Gounaris & Dimarogonas (1988) and Gounaris, Papadoupolos & Dimarogonas (1996)) or the Myklestad approach Mahmoud, Zaid & Al Harashani (1999).

In the development of these theoretical models, it is assumed that the crack remains open during the vibration period. However, unless a static preload exists, during vibrations of the beam the state of stress in the cracked section varies from tension to compression, i.e. the crack opens and closes with time. This results in a modification of the crack section stiffness, the extremal values being the stiffness of the open crack and that of the intact beam. Thus, the non-linear behavior of the closing crack introduces characteristics of the non-linear systems. However, for many practical applications, the system can be considered bilinear, and the fatigue crack can be introduced in the form of the so-called "breathing crack" model which opens when the normal strain near the crack tip is positive, otherwise it closes. The vibration of a beam with a closing crack has been studied in several works: in Chondros & Dimarogonas (2001) and Shen & Chu (1992) a continuous cracked beam theory is assumed and Galerkin procedures are applied; in Sundermeyer & Weaver (1995) a lumped flexibility theory is used and semi-analytical solutions are presented; in Qian, Gu & Jiang (1990), Ruotolo, Surace, Crespo & Storer (1996) and Pugno, Surace & Ruotolo (2000) a finite element model of the cracked beam is used, where reduced stiffness of an element accounts for the crack's presence by "smearing" the crack effect on an entire element; in Luzzato (2003) a "smeared crack" model is compared with a finite element solution of a lumped flexibility model.

In the present paper we propose an accurate numerical technique for the analysis of a beam with multiple cracks based on a meshless local Bubnov-Galerkin formulation of the beam problem. Adopting the lumped flexibility approach, each fatigue crack is modelled as a rotational spring and several damage scenarios are addressed. We study the modal characteristics of a beam with multiple open cracks and its transient behavior when the cracks are breathing.

Meshless methods such as the element-free Galerkin (Belytschko, Lu & Gu (1994)) , hp- clouds (Duarte & Oden (1996)), the reproducing kernel particle (Liu, Jun & Zhang (1995)), the smoothed particle hydrodynamics (Lucy (1977)), the diffuse element (Nayroles, Touzot & Villon (1992)), the partition of unity finite element (Melenk & Babuska (1996)), the natural element (Sukumar, Moran & Belytschko (1998)), meshless Galerkin using radial basis functions (Wendland (1995)), the meshless local Petrov-Galerkin (MLPG) (Atluri & Zhu (1998)), and the modified smoothed particle hydrodynamics (MSPH) (Zhang & Batra (2004)), and the collocation method using multiquadrics basis functions (Kansa (1990); Ferreira, Batra, Roque, Qian & Martins (2005)) for seeking approximate solutions of partial differential equations have become popular during the last two decades because of the flexibility of placing nodes at arbitrary locations and the ability to treat moving boundaries. All of these methods, except for the MLPG, the collocation, and the MSPH, are not truly meshless since the use of shadow elements is inevitable for the integration of the governing weak formulations (Atluri & Shen (2002)). Recent literature (Atluri, Cho & Kim (1999) and Raju & Phillips (2003)) shows increasing interest in the analysis of beams by the use of MLPG methods.

In Atluri, Cho & Kim (1999) the static analysis of thin beams is presented using a Bubnov-Galerkin implementation of the MLPG method (named MLPG6 variant in Atluri & Shen (2002)), i.e. the trial and the test functions are chosen from the same space. In particular, the conventional Moving Least Squares (MLS) approximation presented in Lancaster & Salkauskas (1981) is generalized to treat 4-th order boundary value problems and the resulting Generalized Moving Least Squares (GMLS) approximation is used to construct simultaneously the test and the trial functions. In Raju & Phillips (2003) the static analysis of thin beams is addressed by the use of a Petrov-Galerkin implementation of MLPG method, where the trial functions are constructed using the GMLS approximation and the test functions are chosen from a different space. The GMLS basis functions are generally continuously differentiable over the entire domain which results in continuous derivatives of the trial solution. Thus the treatment of cracked beams necessitates the use of special techniques to account for the slope discontinuities at the crack stations (a similar problem has been studied in Batra, Porfiri & Spinello (2004) for heat conduction in a bimaterial body). In the present paper we use the MLPG6 variant and adopt a substructure approach, by making use of Lagrange multipliers to model the spring effects at the crack locations and relate deformations of the intact beam segments. Warlock, Ching, Kapila & Batra (2002) employed the method of Lagrange multipliers to enforce traction boundary conditions at a rough contact surface, and Batra and Wright (1986) have used it to enforce the non-interpenetration condition at a smooth contact surface.

The paper is organized as follows:

- In Section 2 we review the basic formulation of the GMLS basis functions introduced in Atluri, Cho & Kim (1999).
- In Section 3 we study the dynamics of a multiply cracked beam with the MLPG method. The presence of cracks is accounted for by the introduction of suitable Lagrange multipliers, which guarantee the deflection continuity at the crack locations. The static deformations, the transient behavior and the modal properties are considered in the analysis. The stability of the mixed formulation is discussed and the inf-sup condition is proved.
- In Section 4 we consider effects of cracks opening and closing during the beam vibration period; i.e. we consider the transient analysis of a beam with breathing cracks.
- In Section 5 we report results of numerical experiments, and compare present results with those from other numerical methods, exact solutions and/or experimental findings. Indeed, we compare the finite element and meshless methods in the analysis of static deformations and in the estimation of the modal properties, and we compare the meshless method with the method proposed in Sundermeyer & Weaver (1995) for the analysis of the transient deformations of a beam with breathing cracks.

For the sake of brevity, the approach is presented for a simply supported beam, although it has been found suitable also for other boundary conditions.

2 Generalized Moving Least Squares (GMLS) Basis Functions

Meshless methods generally require local interpolation to represent the trial function. Here we use the generalized moving least squares approximation developed in Atluri, Cho & Kim (1999). This technique generalizes that proposed in Lancaster & Salkauskas (1981) by allowing for the accurate reconstruction of a given trial function on the entire domain, from the knowledge of its values and of its first derivatives at some, suitably chosen, scattered points.

Consider the one-dimensional function w having continuous first derivative on the domain Ω. The (fictitious) nodal values and (fictitious) derivatives at the scattered points $\mathsf{N} = \{x_1, x_2, ..., x_N\}$ in Ω are collected into the two N-vectors $\hat{\mathbf{w}} = [\hat{w}_1, ..., \hat{w}_N]^{\mathrm{T}}$ and $\hat{\vartheta} = [\hat{\vartheta}_1, ..., \hat{\vartheta}_N]^{\mathrm{T}}$ respectively, where the superscript T indicates transposition. The global approximation w^h on Ω is defined as

$$w(x) \simeq w^h(x) = \mathbf{p}^{\mathrm{T}}(x)\,\mathbf{a}(x), \quad x \in \Omega, \tag{1}$$

where

$$\mathbf{p}^{\mathrm{T}}(x) = \left[1, x, x^2, ..., x^{m-1}\right] \tag{2}$$

is a complete monomial basis of degree $m-1$.

The m-vector $\mathbf{a}(x) = [a_1(x), ..., a_m(x)]^{\mathrm{T}}$ is composed of indeterminate coefficients, which vary with the abscissa

x on the domain Ω. At each location $\overline{x}$ on Ω these coefficients are determined by a local least square approximation of $w(x)$ on a small neighborhood $\Omega_{\overline{x}}$ of $\overline{x}$. The local approximation $w_{\overline{x}}(x)$ is defined by

$$w(x) \simeq w_{\overline{x}}(x) = \mathbf{p}^{\mathrm{T}}(x)\,\mathbf{a}(\overline{x}), \quad x \in \Omega_{\overline{x}} \subset \Omega. \tag{3}$$

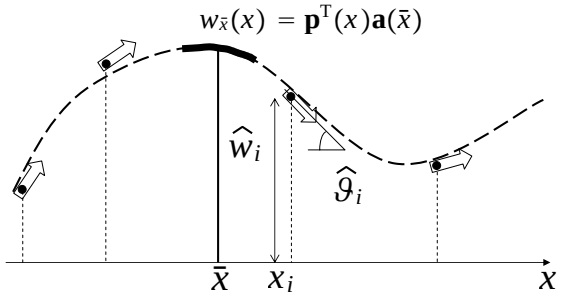

Figure 1 : Sketch of the GMLS approximation.

In a small neighborhood of a generic point $\overline{x}$ the coefficients a_i are treated as the unknown constants of a classical polynomial least square approximation. Therefore, they are determined by minimizing the functional $J_{\overline{x}}$ representing the weighted discrete H^1 error norm (see Atluri, Cho & Kim (1999); and defined by

$$J_{\overline{x}}(\mathbf{a}) = \sum_{i=1}^{N} W_i^{(w)}(\overline{x})\left[w_{\overline{x}}(x_i) - \hat{w}_i\right]^2 + \sum_{i=1}^{N} W_i^{(\vartheta)}(\overline{x})\left[w'_{\overline{x}}(x_i) - \hat{\vartheta}_i\right]^2, \tag{4}$$

where the superimposed prime indicates derivative with respect to the x coordinate. Functions $W_i^{(w)}$ and $W_i^{(\vartheta)}$ are weight functions of node i and are characterized by the following properties: (i) they are continuous, (ii) they equal one at $x = x_i$, (iii) they vanish when $x \notin \left(x_i - R_i^{(w)}, x_i + R_i^{(w)}\right)$ and $x \notin \left(x_i - R_i^{(\vartheta)}, x_i + R_i^{(\vartheta)}\right)$, respectively, and are positive elsewhere. The parameters $R_i^{(w)}$ and $R_i^{(\vartheta)}$ measure semi-supports of the weight functions $W_i^{(w)}$ and $W_i^{(\vartheta)}$ respectively, Figure 1 shows the GMLS approximation.

At a given location $\overline{x}$ only a few terms in summation (4) do not vanish since the supports $R_i^{(w)}$ and $R_i^{(\vartheta)}$ of the weight functions $W_i^{(w)}$ and $W_i^{(\vartheta)}$ are much smaller than the size of Ω. This is used to reduce the memory allocations when implementing the algorithm in a computer code. Lower bounds of $R_i^{(w)}$ and $R_i^{(\vartheta)}$ are stated in Atluri, Cho & Kim (1999) for assuring the regularity of the GMLS basis functions.

The stationarity of $J_{\overline{x}}$ with respect of $\mathbf{a}$ yields

$$\mathbf{A}(\overline{x})\,\mathbf{a}(\overline{x}) = \mathbf{B}(\overline{x}) \begin{bmatrix} \hat{\mathbf{w}} \\ \hat{\vartheta} \end{bmatrix}, \tag{5}$$

where the (m,m) and the (m,N) matrices $\mathbf{A}$ and $\mathbf{B}$ are defined by

$$\begin{aligned} \mathbf{A}(\overline{x}) &= \mathbf{P}^{\mathrm{T}}\mathbf{W}^{(w)}(\overline{x})\,\mathbf{P} + \left(\mathbf{P}'\right)^{\mathrm{T}}\mathbf{W}^{(\vartheta)}(\overline{x})\,\mathbf{P}', \\ \mathbf{B}(\overline{x}) &= \begin{bmatrix} \mathbf{P}^{\mathrm{T}}\mathbf{W}^{(w)}(\overline{x}) & \left(\mathbf{P}'\right)^{\mathrm{T}}\mathbf{W}^{(\vartheta)}(\overline{x}) \end{bmatrix}. \end{aligned} \tag{6}$$

Here $\mathbf{W}^{(w)}$ and $\mathbf{W}^{(\vartheta)}$ are (N,N) diagonal matrices defined by

$$\begin{aligned} \mathbf{W}^{(w)}(\overline{x}) &= \mathrm{DIAG}\begin{bmatrix} W_1^{(w)}(\overline{x}) & \ldots & W_N^{(w)}(\overline{x}) \end{bmatrix}, \\ \mathbf{W}^{(\vartheta)}(\overline{x}) &= \mathrm{DIAG}\begin{bmatrix} W_1^{(\vartheta)}(\overline{x}) & \ldots & W_N^{(\vartheta)}(\overline{x}) \end{bmatrix}, \end{aligned}$$

and $\mathbf{P}$, $\mathbf{P}'$ are (N,m) matrices of real numbers defined by

$$\begin{aligned} \mathbf{P}^{\mathrm{T}} &= \begin{bmatrix} \mathbf{p}(x_1) & \ldots & \mathbf{p}(x_N) \end{bmatrix}, \\ \left(\mathbf{P}'\right)^{\mathrm{T}} &= \begin{bmatrix} \mathbf{p}'(x_1) & \ldots & \mathbf{p}'(x_N) \end{bmatrix}. \end{aligned}$$

Solving (5) for $\mathbf{a}(\overline{x})$ and substituting for $\mathbf{a}(\overline{x})$ in the global approximation (3) we obtain the GMLS approximation

$$w^h(x,t) = \psi^{(w)}(x)^{\mathrm{T}}\hat{\mathbf{w}} + \psi^{(\vartheta)}(x)^{\mathrm{T}}\hat{\vartheta}, \tag{7}$$

where the vectors of basis functions $\psi^{(w)}(x)$ and $\psi^{(\vartheta)}(x)$ are given by

$$\begin{aligned} \psi^{(w)} &= \mathbf{p}(x)^{\mathrm{T}}\mathbf{A}^{-1}(x)\,\mathbf{P}^{\mathrm{T}}\mathbf{W}^{(w)}(x), \\ \psi^{(\vartheta)} &= \mathbf{p}^{\mathrm{T}}(x)\,\mathbf{A}^{-1}(x)\left(\mathbf{P}'\right)^{\mathrm{T}}\mathbf{W}^{(\vartheta)}(x). \end{aligned} \tag{8}$$

It is convenient to group the nodal variables and the GMLS basis functions in the $2N$-vectors $\hat{\mathbf{s}}$ and ψ, respectively.

The smoothness of the GMLS trial functions is completely determined by the smoothness of the weight functions, since the monomial basis is infinitely differentiable. If $\alpha - 1$ indicates the minimum order of differentiability of all weight functions, then from (6) and (8)

it is evident that the trial functions will be at least $\alpha-1$ times differentiable.

In the present work, following Atluri, Cho & Kim (1999) and Raju & Phillips (2003), we assume the same $C^{\alpha-1}(\Omega)$ structure for all weight functions and no distinction is made between the deflection and the rotation weight functions, namely

$$W_i^{(w)}(x) = W_i^{(\vartheta)}(x) = \begin{cases} \left(1-\left(\frac{x-x_i}{R_i}\right)^2\right)^{\alpha} & \text{if } x \in (x_i-R_i, x_i+R_i) \\ 0 & \text{if } x \notin (x_i-R_i, x_i+R_i) \end{cases} . \quad (9)$$

In the analysis of thin beams with the meshless local Bubnov-Galerkin method, we need derivatives of the GMLS basis functions (8). The derivatives of the inverse of the matrix $\mathbf{A}$ are computed from the identity:

$$\mathbf{A}\mathbf{A}^{-1} = \mathbf{1}.$$

Hence

$$\begin{aligned} \left(\mathbf{A}^{-1}\right)' &= -\mathbf{A}^{-1}\mathbf{A}'\mathbf{A}^{-1} \\ \left(\mathbf{A}^{-1}\right)'' &= 2\mathbf{A}^{-1}\mathbf{A}'\mathbf{A}^{-1}\mathbf{A}'\mathbf{A}^{-1} - \mathbf{A}^{-1}\mathbf{A}''\mathbf{A}^{-1} \end{aligned} .$$

Therefore, only the knowledge of the weight functions and their derivatives is needed to compute the derivatives of $\mathbf{A}^{-1}$.

3 Vibrations of a multiply cracked beam

3.1 Governing equations

A beam of length l, cross-sectional area $A = h \times b$, moment of inertia $I = bh^3/12$, Young's modulus E, mass density per unit volume ρ_V with n cracks located at points c_1,..., c_n is considered. The simplest way to account, with a reasonable accuracy, for effects of cracks on the dynamic properties of a slender beam is to represent cracks as lumped flexibility elements and to model the intact regions as Euler-Bernoulli beams. Therefore, following Gudmunson (1983) and Chondros & Dimarogonas (1998) cracks are modelled as n massless rotational springs whose stiffnesses are denoted by k_i. As a consequence, we divide the beam into $n+1$ sub-intervals $\Omega_i = [c_{i-1}, c_i]$ ($c_0 \equiv 0$ and $c_{n+1} \equiv l$) of length l_i, introduce the $n+1$ local abscissas ξ_i and consider $n+1$ deflection fields $w_i(\xi_i)$. Figure 2 exhibits the geometry of the cracked beam.

The vibrations of each undamaged beam segment are governed by

$$K_M w_i^{IV}(\xi_i,t) + \rho\, \ddot{w}_i(\xi_i,t) = p_i(\xi_i,t), \quad \xi_i \in (0,l_i), \quad t>0, \quad (10)$$

where the rotatory inertia has been neglected and $p_i(\xi_i,t)$ indicates an applied distributed transverse load and superimposed dot means time derivative. The boundary conditions for the generic $i-th$ subinterval are

$$\begin{cases} w_i(l_i,t) = w_{i+1}(0,t), \\ w_i''(l_i,t) = w_{i+1}''(0,t), \\ w_i'''(l_i,t) = w_{i+1}'''(0,t), \\ w_i''(l_i,t) = -\dfrac{k_i}{K_M}\left(w_{i+1}'(0,t) - w_i'(l_i,t)\right) \end{cases} . \quad (11)$$

For the two boundary elements Ω_1 and Ω_{n+1} the following additional constraints are imposed:

$$\begin{cases} w_1(0,t) = 0, \quad w_1''(0,t) = 0, \\ w_{n+1}(l_{n+1},t) = 0, \quad w_{n+1}''(l_{n+1},t) = 0 \end{cases} .$$

Following Chondros & Dimarogonas (1998), values of the rotational spring constants k_i can be found from the section geometry, the crack depth a_i and the material properties:

$$k_i = \frac{1}{\alpha_i}, \quad \alpha_i = \frac{6\pi(1-\nu^2)}{EI} I_c\left(\frac{a_i}{h}\right)$$

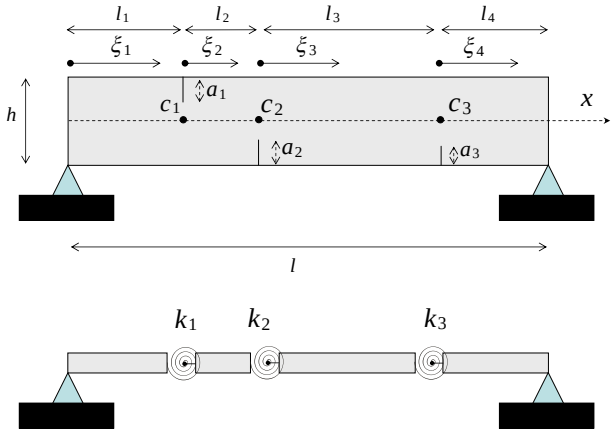

Figure 2 : Sketch of a cracked beam and of its lumped flexibility model.

where ν is the Poisson ratio and

$$I_c(z) = 0.6272z^2 - 1.04533z^3 + 4.5948z^4 - 9.9736z^5 + 20.2948z^6 - 33.0251z^7 + 47.1063z^8 - 40.7556z^9 + 19.6z^{10},$$

with z indicating severity of the i-th crack. This modeling technique provides reasonable results as long as cracks remain open during the vibration period. The crack opening and closing (breathing crack) introduce weak nonlinearities in the beam motion and modify natural frequencies of vibrations. In the following section we analyze the effect of breathing cracks by a meshless method together with a classical time integration scheme.

3.2 Semi-discrete formulation

In order to derive a weak formulation of the aforementioned fourth-order problem suitable for numerical methods, we introduce the augmented Lagrangian, that is a function of the deflection fields w_i in the undamaged beam segments, and the Lagrange multipliers λ_i:

$$\begin{aligned} &L(w_1,...,w_{n+1},\lambda_0,...,\lambda_{n+1}) \\ &= \frac{1}{2}\sum_{i=1}^{n+1}\int_0^{l_i}\left[\rho\dot{w}_i^2 - K_M\left(w_i''\right)^2 + 2p_iw_i\right]d\xi_i \\ &- \frac{1}{2}\sum_{i=1}^{n}k_i\left(w_{i+1}'(0) - w_i'(l_i)\right)^2 \\ &- \sum_{i=1}^{n}\lambda_i\left(w_{i+1}(0) - w_i(l_i)\right) \\ &- \lambda_0 w_1(0) - \lambda_{n+1}w_{n+1}(l_{n+1}), \end{aligned} \tag{12}$$

where we have omitted the dependence on time of the deflection fields, Lagrange multipliers and applied load. The Lagrange multipliers λ_0 and λ_{n+1} are used to impose the displacement boundary conditions at the ends, while the other Lagrange multipliers impose the continuity of deflections at the crack locations. We emphasize that the proposed formulation leads to continuous deflections along the entire beam span. On the other hand, the continuity of the bending moments and of the shear forces at the crack locations are satisfied only approximately. By extremizing the Action on the set of isochronous motions we obtain

$$\begin{aligned} &\sum_{i=1}^{n+1}\int_0^t\int_0^{l_i}\left[\rho\ddot{w}_i\delta w_i + K_M w_i''\delta w_i'' - p_i w_i\right]d\xi_i dt \\ &+ \sum_{i=1}^{n}k_i\left(w_{i+1}'(0) - w_i'(l_i)\right)\left(\delta w_{i+1}'(0) - \delta w_i'(l_i)\right) \\ &+ \int_0^t\left[\begin{array}{l}\lambda_0\delta w_1(0) + \lambda_{n+1}\delta w_{n+1}(l_{n+1}) \\ +\sum_{i=1}^{n}\lambda_i\left(\delta w_{i+1}(0) - \delta w_i(l_i)\right)\end{array}\right]dt \\ &+ \int_0^t\left[\begin{array}{l}\delta\lambda_0 w_1(0) + \delta\lambda_{n+1}w_{n+1}(l_{n+1}) \\ +\sum_{i=1}^{n}\delta\lambda_i\left(w_{i+1}(0) - w_i(l_i)\right)\end{array}\right]dt \\ &= 0. \end{aligned} \tag{13}$$

Next, we consider $n+1$ distinct sets of scattered points $N_i = \left\{\xi_{i_1},...,\xi_{i_{N_i}}\right\}$ with $\xi_{i_1} = 0$, $\xi_{i_{N_i}} = l_i = \xi_{(i+1)_1}$, for the subintervals Ω_i, and derive independently $n+1$ distinct set of basis functions $\psi_i(\xi_i)$ of the type (8). We denote with N the total number of nodes scattered on the entire beam and we emphasize that at each crack location two overlapping nodes are placed. For convenience, these trial functions are derived by assuming for each subinterval the same order for the monomial basis functions in the GMLS approximation and the same form of the weight functions (9). Furthermore, we denote by R_{i_j} the radius of the support of the *j-th* weight function of the *i-th* subdomain. We consider test functions of the form:

$$\delta w_i = \psi_i(\xi_i)^{\mathrm{T}}\mu_i,$$

where μ_i is a $2N_i$-vector of arbitrary constants.

By substituting in (13) the GMLS approximation together with the considered test functions and by accounting for the arbitrariness of the real constants μ_i's we obtain the following semi-discrete formulation

$$\begin{cases} \mathbf{M}\ddot{\hat{\mathbf{s}}} + \mathbf{K}\hat{\mathbf{s}} + \Lambda\lambda = \mathbf{F} \\ \Lambda^{\mathrm{T}}\hat{\mathbf{s}} = \mathbf{0} \end{cases}. \tag{14}$$

The generalized displacement vector is comprised of nodal displacements and rotations in all segments of the beam:

$$\hat{\mathbf{s}} = \left[\begin{array}{cccccc}\hat{\mathbf{s}}_1 & \cdots & \hat{\mathbf{s}}_i & \cdots & \hat{\mathbf{s}}_{n+1}\end{array}\right]^{\mathrm{T}}.$$

The mass matrix $\mathbf{M}$ is a symmetric nonnegative definite

block diagonal matrix

$$\mathbf{M} = \begin{bmatrix} \mathbf{m}_1 & \mathbf{0} & \cdots & \mathbf{0} \\ \mathbf{0} & \mathbf{m}_2 & \mathbf{0} & \cdots \\ \cdots & \mathbf{0} & \cdots & \cdots \\ \mathbf{0} & \cdots & \cdots & \mathbf{m}_{(n+1)} \end{bmatrix},$$

with

$$\mathbf{m}_i = \rho \int_{\Omega_i} \psi_i \left(\psi_i\right)^{\mathrm{T}} d\xi_i. \tag{15}$$

Therefore, the beam segments are inertially uncoupled by the lumped flexibilities appearing in the cracked beam model but are elastically coupled.

The symmetric nonnegative definite stiffness matrix can be decomposed as

$$\mathbf{K} = \mathbf{K}^0 + \sum_{i=1}^{n} \mathbf{K}_i^{spr},$$

where the block-diagonal stiffness contribution $\mathbf{K}^0$ is obtained from the segments stiffness matrices following the same procedure as that used for assembling of $\mathbf{M}$ from the segments mass matrices:

$$\mathbf{K} = \begin{bmatrix} \mathbf{k}_1 & \mathbf{0} & \cdots & \mathbf{0} \\ \mathbf{0} & \mathbf{k}_2 & \mathbf{0} & \cdots \\ \cdots & \mathbf{0} & \cdots & \cdots \\ \mathbf{0} & \cdots & \cdots & \mathbf{k}_{(n+1)} \end{bmatrix},$$

with

$$\mathbf{k}_i = K_M \int_{\Omega_i} \left(\psi_i\right)'' \left(\left(\psi_i\right)''\right)^{\mathrm{T}} d\xi_i. \tag{16}$$

On the other hand, the contribution of the i-th crack to the beam stiffness $\mathbf{K}_i^{spr}$ has non-zero entries only in correspondence of the i-th and $(i+1)$-th beam segments, i.e.:

$$\mathbf{K}_i^{spr} = k_i \begin{bmatrix} \mathbf{0} & \cdots & \cdots & \cdots & \cdots & \mathbf{0} \\ \cdots & \cdots & \cdots & \cdots & \cdots & \cdots \\ \cdots & \cdots & \mathbf{A}_i & \mathbf{B}_i & \cdots & \cdots \\ \cdots & \cdots & \mathbf{B}_i^{\mathrm{T}} & \mathbf{C}_i & \cdots & \cdots \\ \cdots & \cdots & \cdots & \cdots & \cdots & \cdots \\ \mathbf{0} & \cdots & \cdots & \cdots & \cdots & \mathbf{0} \end{bmatrix},$$

where matrices $\mathbf{A}_i$, $\mathbf{B}_i$ and $\mathbf{C}_i$ are are given by

$$\mathbf{A}_i = \left(\psi_i\right)'(l_i) \left(\left(\psi_i\right)'(l_i)\right)^{\mathrm{T}},$$
$$\mathbf{B}_i = -\left(\psi_i\right)'(l_i) \left(\left(\psi_{i+1}\right)'(0)\right)^{\mathrm{T}},$$
$$\mathbf{C}_i = \left(\psi_{i+1}\right)'(0) \left(\left(\psi_{i+1}\right)'(0)\right)^{\mathrm{T}}.$$

The constraint matrix Λ is assembled by appending the column vectors

$$\Lambda = \begin{bmatrix} \Lambda_0 & \Lambda_1 & \cdots & \Lambda_i & \cdots & \Lambda_n & \Lambda_{n+1} \end{bmatrix},$$

where

$$\Lambda_0 = \begin{bmatrix} \mathbf{a}_0 \\ \mathbf{0} \\ \cdots \\ \mathbf{0} \end{bmatrix}, \quad \Lambda_i = \begin{bmatrix} \mathbf{0} \\ \cdots \\ \mathbf{a}_i \\ \mathbf{b}_i \\ \mathbf{0} \\ \cdots \\ \mathbf{0} \end{bmatrix}, \quad \Lambda_{n+1} = \begin{bmatrix} \mathbf{0} \\ \mathbf{0} \\ \cdots \\ \mathbf{b}_{n+1} \end{bmatrix}.$$

The column vectors with subscripts 0 and $n+1$ arise from the need to satisfy displacement boundary conditions, while the one with subscript i is due to the i-th crack. The subvectors are related to the test and the trial functions as

$$\mathbf{a}_0 = \psi_1(0), \qquad \mathbf{a}_i = -\psi_i(l_i),$$
$$\mathbf{b}_i = \psi_{i+1}(0), \qquad \mathbf{b}_{n+1} = \psi_{n+1}(l_{n+1}).$$

Finally, the force vector $\mathbf{F}$ is:

$$\mathbf{F} = \begin{bmatrix} \mathbf{f}_1 & \cdots & \mathbf{f}_i & \cdots & \mathbf{f}_{n+1} \end{bmatrix}^{\mathrm{T}}$$

with

$$\mathbf{f}_i = \int_{\Omega_i} p_i \psi_i d\xi_i. \tag{17}$$

3.3 *Inf-sup test*

In order to achieve a stable and optimal procedure for the MLPG method employing a set of Lagrange multipliers, the considered mixed formulation for static problems should satisfy the ellipticity condition (on the space of displacement fields satisfying the kinematic boundary conditions) and the inf-sup condition (Bathe (1996)). For this linear problem the ellipticity condition is readily satisfied, while additional effort is needed to provide criteria for satisfying the inf-sup condition, which reads:

$$\inf_{\lambda \in \mathbb{R}^{n+2}} \sup_{w^h \in W^h} \frac{\begin{bmatrix} \lambda_0 w_1^h(0) + \lambda_{n+1} w_{n+1}^h(l_{n+1}) \\ + \sum_{i=1}^{n} \lambda_i \left(w_{i+1}^h(0) - w_i^h(l_i)\right) \end{bmatrix}}{\|\lambda\| \, \|w^h\|} \geq \beta > 0,$$

where $w^h \neq 0$, $\beta \neq 0$, β is a constant independent of the nodal locations and $W^h \subset H^2(0,l_1) \times ... \times H^2(0,l_n)$ is the GMLS solution space. The norm of the approximate deflection field is defined by:

$$\left\|w^h\right\|^2 = \sum_{i=1}^{n+1} \int_0^{l_i} \left[\begin{array}{l} \left(w_i^h\right)^2 + l^2 \left(\left(w_i^h\right)'\right)^2 \\ +l^4 \left(\left(w_i^h\right)''\right)^2 \end{array} \right] d\xi_i$$

while the norm of the vector of scalars λ is

$$\|\lambda\|^2 = \lambda^{\mathrm{T}}\lambda.$$

When these two conditions are satisfied, the stability of the MLPG formulation is guaranteed and optimal error bounds are obtained for the chosen GMLS solution.

We show below that the inf-sup condition is satisfied when m, the order of the monomial basis in (2), is greater than 1. Indeed, in this case the GMLS approximation is able to exactly reproduce affine functions (see (3) when $\mathbf{a}(\overline{x})$ is a constant). Therefore, for a typical λ, we choose deflection fields of the form

$$\left\{ \begin{array}{l} \overline{w}_i^h(\xi_i) = \lambda_{i-1}\left(1 - \frac{\xi_i}{l_i}\right), \qquad i = 1,...,n \\ \overline{w}_{n+1}^h(\xi_i) = \lambda_n + \dfrac{\lambda_{n+1} - \lambda_n}{l_{n+1}} \xi_{n+1} \end{array} \right. . \tag{18}$$

The norm of this deflection is easily computed as:

$$\begin{aligned} \left\|\overline{w}^h\right\|^2 = & \sum_{i=1}^{n+1} \lambda_{i-1}^2 \left(\frac{l_i}{3} + \frac{l^2}{l_i}\right) + \lambda_{n+1}^2 \left(\frac{l_{n+1}}{3} + \frac{l^2}{l_{n+1}}\right) \\ & + \lambda_{n+1}\lambda_n \left(\frac{l_{n+1}}{3} - 2\frac{l^2}{l_{n+1}}\right). \end{aligned} \tag{19}$$

Equation (19) may be alternatively rewritten in matrix notation as:

$$\left\|\overline{w}^h\right\|^2 = \lambda^{\mathrm{T}}\mathbf{S}\lambda,$$

where the $(n+2)(n+2)$ matrix $\mathbf{S}$, defined by

$$\mathbf{S} = \left[\begin{array}{ccccc} \left(\frac{l_1}{3} + \frac{l^2}{l_1}\right) & 0 & \cdots & & \\ 0 & \left(\frac{l_2}{3} + \frac{l^2}{l_2}\right) & 0 & & \\ \cdots & 0 & \cdots & & \\ 0 & 0 & 0 & & \\ 0 & \cdots & \cdots & & \\ & \cdots & & 0 & \\ & \cdots & & 0 & \\ & \cdots & & \cdots & \\ & \left(\frac{l_{n+1}}{3} + \frac{l^2}{l_{n+1}}\right) & & \frac{1}{2}\left(\frac{l_{n+1}}{3} - 2\frac{l^2}{l_{n+1}}\right) & \\ & \frac{1}{2}\left(\frac{l_{n+1}}{3} - 2\frac{l^2}{l_{n+1}}\right) & & \left(\frac{l_{n+1}}{3} + \frac{l^2}{l_{n+1}}\right) & \end{array} \right], \tag{20}$$

appears. The eigenvalues $\sigma_1, ..., \sigma_{n+2}$ of $\mathbf{S}$ are:

$$\sigma_i = \left(\frac{l_i}{3} + \frac{l^2}{l_i}\right), \qquad i = 1,...,n,$$

$$\sigma_{n+1} = \frac{l_{n+1}}{2}, \qquad \sigma_{n+2} = \frac{l_{n+1}}{6} + 2\frac{l^2}{l_{n+1}}.$$

Hence $\mathbf{S}$ is a positive definite matrix and

$$\max\sigma_i \|\lambda\|^2 \geq \left\|\overline{w}^h\right\|^2 \geq \min\sigma_i \|\lambda\|^2.$$

By substituting (18) in the argument of the inf-sup we obtain

$$\frac{\left[\begin{array}{l} \lambda_0 \overline{w}_1^h(0) + \lambda_{n+1}\overline{w}_{n+1}^h(l_{n+1}) \\ +\sum_{i=1}^{n} \lambda_i \left(\overline{w}_{i+1}^h(0) - \overline{w}_i^h(l_i)\right) \end{array} \right]}{\|\lambda\| \left\|\overline{w}^h\right\|} = \frac{\|\lambda\|}{\sqrt{\lambda^{\mathrm{T}}\mathbf{S}\lambda}}.$$

Hence, we have

$$\sup_{w^h \in W^h} \frac{\left[\begin{array}{l} \lambda_0 w_1^h(0) + \lambda_{n+1} w_{n+1}^h(l_{n+1}) \\ +\sum_{i=1}^{n} \lambda_i \left(w_{i+1}^h(0) - w_i^h(l_i)\right) \end{array} \right]}{\|\lambda\| \|w^h\|} \geq \frac{\|\lambda\|}{\sqrt{\lambda^{\mathrm{T}}\mathbf{S}\lambda}}$$

with λ still a variable. Therefore, for the mixed GMLS approximation with $m > 1$, $w^h \neq 0$, $\lambda \neq 0$, we have

$$\begin{aligned} & \inf_{\lambda \in \mathbb{R}^{n+2}} \sup_{w^h \in W^h} \frac{\left[\begin{array}{l} \lambda_0 w_1^h(0) + \lambda_{n+1} w_{n+1}^h(l_{n+1}) \\ +\sum_{i=1}^{n} \lambda_i \left(w_{i+1}^h(0) - w_i^h(l_i)\right) \end{array} \right]}{\|\lambda\| \|w^h\|} \\ & \geq \inf_{\lambda \in \mathbb{R}^{n+2}} \frac{\|\lambda\|}{\sqrt{\lambda^{\mathrm{T}}\mathbf{S}\lambda}} = \frac{1}{\sqrt{\max\sigma_i}}, \end{aligned} \tag{21}$$

and the inf-sup condition is satisfied.

3.4 Modal Analysis

The natural frequencies and mode shapes of the undamaged beam are obtained by searching for solutions of the type

$$\hat{\mathbf{s}}(t) = \check{\mathbf{s}}\exp(i\omega t), \quad \lambda(t) = \check{\lambda}\exp(i\omega t),$$

of (14) and by discarding the applied loads. Therefore, the following eigenvalue problem arises:

$$\left\{ \begin{array}{l} -\omega^2\mathbf{M}\check{\mathbf{s}} + \mathbf{K}\check{\mathbf{s}} + \Lambda\check{\lambda} = \mathbf{0} \\ \Lambda^{\mathrm{T}}\check{\mathbf{s}} = \mathbf{0} \end{array} \right. . \tag{22}$$

Equation $(22)_2$ provides $2+n$ constraints on the mode shapes $\check{\mathbf{s}}$.We modify the eigenvalue problem (22) so that the imposed constraints are automatically satisfied.

Let us consider the *null space* of Λ^{T}, denoted by $\ker\Lambda^{\mathrm{T}}$. When the inf-sup condition is satisfied the dimension of the kernel of Λ^{T} is

$$\dim\ker\Lambda^{\mathrm{T}} = (2N-2-n),$$

since $2+n$ Lagrange multipliers appear in this formulation and the system is solvable (see Bathe (1996) for a discussion of the relations between solvability and stability conditions). Next, we introduce the matrix $\mathbf{Y}$ whose columns constitute a basis for $\ker\Lambda^{\mathrm{T}}$, the dimensions of $\mathbf{Y}$ are $(2N\times(2N-2-n))$. By using the rectangular matrix $\mathbf{Y}$ we can express the generic modal shape $\check{\mathbf{s}}$ in terms of the reduced $(2N-2)$-dimensional vector $\mathbf{x}$ by

$$\check{\mathbf{s}} = \mathbf{Y}\mathbf{x}, \tag{23}$$

and automatically satisfy equation $(22)_2$.

Premultiplying $(22)_1$ by $\mathbf{Y}^{\mathrm{T}}$ and by taking into account (23) we obtain the reduced system

$$-\omega^2\mathbf{M}^*\mathbf{x}+\mathbf{K}^*\mathbf{x}=\mathbf{0}$$

where

$$\mathbf{M}^*=\mathbf{Y}^{\mathrm{T}}\mathbf{M}\mathbf{Y},\ \mathbf{K}^*=\mathbf{Y}^{\mathrm{T}}\mathbf{K}\mathbf{Y}.$$

Next, we solve for $\mathbf{x}$, and obtain the complete vector of unknowns using (23). We note that the kinematical boundary conditions are automatically satisfied by the introduction of Lagrange multipliers, while the natural boundary conditions are satisfied only in the weak sense. Furthermore we can always assume that

$$\mathbf{Y}^{\mathrm{T}}\mathbf{Y}=\mathbf{1},$$

by choosing orthonormal basis for the null space of Λ^{T}. We note that the mass and the stiffness matrices of the reduced system are symmetric and positive definite.

3.5 Free motion

We integrate the differential equations of motion (14) with initial conditions

$$\begin{cases} \hat{\mathbf{s}}(0)=\hat{\mathbf{s}}_0 \\ \dot{\hat{\mathbf{s}}}(0)=\dot{\hat{\mathbf{s}}}_0 \end{cases}$$

satisfying the boundary conditions

$$\Lambda^{\mathrm{T}}\hat{\mathbf{s}}_0=\mathbf{0},\quad \Lambda^{\mathrm{T}}\dot{\hat{\mathbf{s}}}_0=\mathbf{0},$$

and vanishing external load, by applying the Newmark family of methods (see e.g. Hughes (1987)) to the reduced system

$$\mathbf{M}^*\ddot{\mathbf{x}}+\mathbf{K}^*\mathbf{x}=\mathbf{0},$$

with initial conditions:

$$\begin{cases} \mathbf{x}(0)=\mathbf{Y}^{\mathrm{T}}\hat{\mathbf{s}}_0 \\ \dot{\mathbf{x}}(0)=\mathbf{Y}^{\mathrm{T}}\dot{\hat{\mathbf{s}}}_0 \end{cases}.$$

This family of algorithms consists of the following recursive relations:

$$\begin{cases} \mathbf{M}^*\mathbf{a}_{n+1}+\mathbf{K}^*\mathbf{x}_{n+1}=\mathbf{0}, \\ \mathbf{x}_{n+1}=\mathbf{x}_n+\Delta t\,\mathbf{v}_n+\dfrac{\Delta t^2}{2}\left[(1-2\beta)\,\mathbf{a}_n+2\beta\mathbf{a}_{n+1}\right], \\ \mathbf{v}_{n+1}=\mathbf{v}_n+\Delta t\left[(1-\gamma)\,\mathbf{a}_n+\gamma\mathbf{a}_{n+1}\right], \end{cases}$$

where $\mathbf{a}_n$, $\mathbf{v}_n$ and $\mathbf{x}_n$ are approximations of $\ddot{\mathbf{x}}(t_n)$, $\dot{\mathbf{x}}(t_n)$ and $\mathbf{x}(t_n)$ respectively, Δt is the time step, and β and γ are parameters.

4 Effects of crack opening and closing

During the vibration period of a cracked beam, the n cracks will open and close in time depending on the vibration amplitude. In order to model the effects of the cracks opening and closing, we consider a bilinear behavior of each crack. When the i-th crack is open, the i-th and $(i+1)$-th beam segments are elastically coupled by the rotational spring k_i (see the continuity conditions (11)). On the other hand, when the i-th crack is closed, the i-th and $(i+1)$-th beam segments are rigidly connected and the boundary conditions become

$$\begin{cases} w_i(l_i,t)=w_{i+1}(0,t), \quad w_i''(l_i,t)=w_{i+1}''(0,t), \\ w_i'''(l_i,t)=w_{i+1}'''(0,t), \quad w_i'(l_i,t)=w_{i+1}'(0,t). \end{cases}.$$

The i-th single edge crack is assumed to be open or closed depending on the sign of the curvature $w_{i+1}''(0,t)$:

- if the crack is on the upper beam surface, the crack is open when the curvature is negative and vice-versa,
- if the crack is on the bottom beam surface, the crack is open when the curvature is positive and vice-versa.

When the i-th crack is closed the augmented Lagrangian (12) needs to be modified by removing the strain energy contribution from the spring k_i and by introducing an additional Lagrange multiplier ζ_i to enforce the continuity of rotations at the crack location. Therefore, the equations of motion of the cracked beam are

$$\begin{cases} \mathbf{M}\ddot{\hat{\mathbf{s}}} + \mathbf{K}^0\hat{\mathbf{s}} + \sum_{i=1}^{n} \delta_i \mathbf{K}_i^{spr}\hat{\mathbf{s}} + \Lambda\lambda + \sum_{i=1}^{n} (1-\delta_i)\Upsilon_i\zeta_i = \mathbf{0} \\ \Lambda^{\mathrm{T}}\hat{\mathbf{s}} = \mathbf{0} \\ (1-\delta_i)\Upsilon_i^{\mathrm{T}}\hat{\mathbf{s}} = \mathbf{0}, \qquad i = 1,\ldots n, \end{cases}, \tag{24}$$

where δ_i is equal to 1 or 0 if the i-th crack is open or closed. The new vector Υ_i is given by

$$\Upsilon_i = \begin{bmatrix} \mathbf{0} & \cdots & \mathbf{c}_i & \mathbf{d}_i & \mathbf{0} & \cdots & \mathbf{0} \end{bmatrix}^{\mathrm{T}},$$

where the subvectors are decomposed by:

$$\mathbf{c}_i = -(\psi_i)'(l_i), \qquad \mathbf{d}_i = (\psi_i)'(0).$$

If q cracks are closed, the number of Lagrange multipliers is $2+n+q$ and the third set of equations in (24) consists of q equations.

The instantaneous values of the δ's depend on the sign of curvature at the crack locations. The aforestated weak formulation does not guarantee continuity of the curvature along the beam span. Therefore, the generic δ_i can be estimated either from the average curvature at the i-th crack location, or from the curvature of any of the two segments.

Vibration cycle is referred to as the time interval between two consecutive sign changes in the curvature at any crack location; the so-called transition time separates two consecutive vibration cycles. During each vibration cycle, labelled by the index τ, the time integration of the non-linear equations of motion can be performed by applying the Newmark family of methods to the reduced equations during the τ-th cycle:

$$\mathbf{M}_\tau^* \ddot{\mathbf{x}}_\tau(t) + \mathbf{K}_\tau^* \mathbf{x}_\tau(t) = \mathbf{0}. \tag{25}$$

The set (25) of linear ordinary differential equations with constant coefficients has been obtained with the same procedure as that used for open cracks, provided that the actual constraints are accounted for during the current vibration cycle τ. Numerical integration gives estimates of transition times only within the accuracy of the time step Δt. If a transition occurs in between the J and $J+1$ integration steps, which separate the vibration cycles τ and $\tau+1$, then the the initial conditions for the $\tau+1$ vibration cycle can be derived as follows:

$$\begin{cases} \mathbf{x}_{\tau+1}(t_{J+1}) = \mathbf{Y}_{\tau+1}{}^{\mathrm{T}}\mathbf{Y}_\tau \mathbf{x}_\tau(t_{J+1}) \\ \mathbf{v}_{\tau+1}(t_{J+1}) = \mathbf{Y}_{\tau+1}{}^{\mathrm{T}}\mathbf{Y}_\tau \mathbf{v}_\tau(t_{J+1}) \end{cases}, \tag{26}$$

where columns of the matrix $\mathbf{Y}_\tau$ constitute an orthonormal basis for $\ker\Lambda_\tau^{\mathrm{T}}$. The left-hand side of equations (26) are the projection of the solution $\mathbf{x}_\tau$ and $\mathbf{v}_\tau$ on the basis of the solution at the subsequent cycle $\mathbf{x}_{\tau+1}$ and $\mathbf{v}_{\tau+1}$.

5 Computation and discussion of results

For investigating the characteristics of the proposed method, several tests are performed on the sample problem of a simply supported beam with a single crack located at the mid-span.

When the beam is subjected to a constant distributed load p, the static deflection is

$$\begin{cases} w_1(\xi_1) = \dfrac{pl^2(2k_1 l + 3K_M)}{48K_M k_1}\xi_1 \\ \qquad\qquad -\dfrac{pl}{12K_M}\xi_1^3 + \dfrac{p}{24K_M}\xi_1^4 \\ w_2(\xi_2) = \dfrac{pl^3(5k_1 l + 12K_M)}{384K_M k_1} \\ \qquad\qquad -\dfrac{pl^2}{16k_1}\xi_2 - \dfrac{pl^2}{16K_M}\xi_2^2 + \dfrac{p}{24K_M}\xi_2^4 \end{cases}.$$

The exact modal properties of a beam with one open crack are given in Sundermeyer & Weaver (1995). The odd wave number, β, is a root of the trascendental characteristic equation:

$$\frac{-4k_1}{K_M}\cos\left(\frac{l\beta}{2}\right) + \beta\left(\sin\left(\frac{l\beta}{2}\right) - \cos\left(\frac{l\beta}{2}\right)\tanh\left(\frac{l\beta}{2}\right)\right) = 0$$

while the even ones are

$$\beta = \frac{r\pi}{l}, \quad r = 2,4,6,\ldots.$$

The odd mode shapes are

$$\begin{cases} w_1(\xi_1) = A\left[\sin(\beta\xi_1) + \alpha\sinh(\beta\xi_1)\right] \\ w_2(\xi_2) = A\begin{bmatrix} \sin\left(\beta\left(\frac{l}{2}-\xi_2\right)\right) \\ +\alpha\sinh\left(\beta\left(\frac{l}{2}-\xi_2\right)\right) \end{bmatrix} \end{cases},$$

$$\alpha = \frac{\cos\left(\frac{l\beta}{2}\right)}{\cosh\left(\frac{l\beta}{2}\right)}, \tag{27}$$

while the even ones are

$$\begin{cases} w_1(\xi_1) = A\sin(\beta\xi_1) \\ w_2(\xi_2) = A\sin(\beta(\xi_2 - l/2)) \end{cases}. \tag{28}$$

The constant A is chosen by ensuring that

$$\int_0^{l/2} (w_1(\xi_1))^2 d\xi_1 + \int_0^{l/2} (w_2(\xi_2))^2 d\xi_2 = 1.$$

The GMLS basis functions are generated by complete monomials of degree 2 ($m = 3$). This choice is motivated by the need of satisfying the inf-sup condition, guaranteeing an accurate GMLS reconstruction and of reducing the computational time. For $m = 3$ the GMLS trial functions require the inversion of a 3×3 matrix, which can be done analytically once for all. Every beam segment is discretized with the same number of nodes $N_1 = N_2$, and the nodal spacing is uniform. The radius of support of each weight function is the same and equals $sl_1/(N_1 - 1) = sl_2/(N_2 - 1)$, where s is the ratio between the weight function radius and the distance between two adjacent nodes. In order to achieve smooth approximate solutions, the power α in equation (9) is set equal to 5. Increasing the order of differentiability of the weight functions does not lead to additional computational effort, therefore it is generally advisable to exploit high values of α. The numerical integrations needed for computing the stiffness matrix, the mass matrix and the load vector are performed using the non-element local technique described in Atluri, Cho & Kim (1999) with 10 quadrature points in each subregion of intersection of sub-domains.

We compare the MLPG results with those obtained from the traditional Finite Element method (FEM), which may be directly derived upon replacing the GMLS approximation with the Hermitian interpolation function (see e.g. Hughes (1987)) in the stiffness matrix, in the mass matrix and in the force vector. We emphasize that within the FEM there is no need to use a mixed formulation based on the introduction of Lagrange multipliers for prescribing the boundary and the interface conditions. The trial functions of the FEM possess the Kronecker Delta property and the constraints are simply imposed by eliminating from the stiffness matrix, the mass matrix and the force vector the entries corresponding to constrained nodes.

We analyze deformations of an aluminum beam with the following values of material and geometric parameters:

$$E = 72\,Gpa, \quad \rho_V = 2800\,kg/m^3, \quad \nu = 0.35,$$
$$l = 235\,mm, \quad h = 23\,mm, \quad b = 7\,mm,$$
$$a_1 = 0.4h.$$

Experiments on this beam, with different crack severities are reported in Chondros & Dimarogonas (1998), Chondros & Dimarogonas (2001) and Chondros (2001).

5.1 Convergence Analysis

Convergence tests are performed for both the analysis of static deformations and modal properties with $s = 4.7$. To observe the convergence, three relative error norms are used. They are defined below, where the superscript h indicates the numerical solution (MLPG or FE) and the superscript *exact* refers to the analytical solution.

- Relative L_2 error norm:
$$\frac{\sqrt{\sum_{i=1}^{2}\int_0^{l_i}\left(w_i^h - w_i^{exact}\right)^2 d\xi_i}}{\sqrt{\sum_{i=1}^{2}\int_0^{l_i}\left(w_i^{exact}\right)^2 d\xi_i}},$$
- Relative H_1 error norm:
$$\frac{\sqrt{\begin{array}{c}\sum_{i=1}^{2}\int_0^{l_i}\left[\left(w_i^h - w_i^{exact}\right)^2\right] d\xi_i \\ +\sum_{i=1}^{2}\int_0^{l_i}\left[l^2\left(\left(w_i^h\right)' - \left(w_i^{exact}\right)'\right)^2\right] d\xi_i\end{array}}}{\sqrt{\sum_{i=1}^{2}\int_0^{l_i}\left[\left(w_i^{exact}\right)^2 + l^2\left(\left(w_i^{exact}\right)'\right)^2\right]}},$$
- Relative H_2 error norm:
$$\frac{\sqrt{\begin{array}{c}\sum_{i=1}^{2}\int_0^{l_i}\left[\left(w_i^h - w_i^{exact}\right)^2\right] d\xi_i \\ -\sum_{i=1}^{2}\int_0^{l_i}\begin{bmatrix} l^2\left(\left(w_i^h\right)' - \left(w_i^{exact}\right)'\right)^2 \\ +l^4\left(\left(w_i^h\right)'' - \left(w_i^{exact}\right)''\right)^2\end{bmatrix} d\xi_i\end{array}}}{\sqrt{\sum_{i=1}^{2}\int_0^{l_i}\left[\left(w_i^{exact}\right)^2 + l^2\left(\left(w_i^{exact}\right)'\right)^2 + l^4\left(\left(w_i^{exact}\right)''\right)^2\right]}}.$$

In Figure 3, we report for static deformations of a beam loaded by a uniformly distributed load on the top surface the error norms for solutions computed with the FE and the meshless methods. The results show that the convergence rates of L_2, H_1 and H_2 error norms for the two methods are almost the same and approximately equal 4, 3 and 2 respectively. In general, the error of the MLPG solution is lower than that of the FE solution.

Figure 4 shows the relative errors in the resonance frequencies of the three lowest vibration modes. Also in this case, the convergence rates for the two methods are almost the same and approximately equal 4. Nevertheless, it may be seen that the magnitude of the error obtained with the meshless approach is less than that with the FEM.

Figures 5, 6 and 7 show respectively the convergence rates of L_2, H_1 and H_2 error norms for the three lowest modes computed with the two numerical methods. The results show that, also in this case, the convergence rates of L_2, H_1 and H_2 error norms for the two methods are almost the same and approximately equal 4, 3 and 2 respectively. The magnitude of the error in the highest modes achieved with the MLPG method is still lower than that obtained with the FEM.

5.2 Variations of weight functions radii

From the above analysis, it is evident that when increasing the number of nodes the MLPG method tends to reach a stable convergence rate similar to the FEM. On the other hand when only a few nodes are employed non monotonic behaviors are exhibited and the MLPG solution is more accurate than the FE solution (see e.g. Figure 4). This is due to the fact that for coarse grids the local feature of the MLPG method is lost and each node is affecting almost all nodes, increasing the computational time for evaluating every matrix entry but also considerably improving the accuracy of the GMLS reconstruction capability.

Here we investigate the behavior of the MLPG solution when the number of nodes in each segment is kept constant (4 nodes per segment) while the radius of the weight functions is increased until each node is affecting all the other ones ($1.5 \leq s \leq 4$).

Figure 8 shows the error in the static deflection computed with the MLPG and the FE methods. It is clear that increasing the radius of the weight functions leads to a significant improvement of the MLPG solution. Indeed, for $s \leq 3$ the FE solution is more accurate than the MLPG one, but when $s > 3$ the situation is completely reversed and the MLPG method gives significantly less errors than the FEM.

Figure 9 shows the error in the four lowest natural frequencies computed with the MLPG and the FE methods. Also in this case, an increase in the weight functions radii leads to a great improvement. Whereas, the error in the first natural frequency monotonically decreases with an increase in the parameter s, the errors in other frequencies do not decrease monotonically; however, they are always much lower (about 100 times) than those for the FE solution.

In Figure 10 we report the ratio of the exact first natural frequency of the intact beam to that of the cracked beam for different values of the crack depth a (solid line) and its approximation by using the $4+4$ nodes configuration with $s = 3$. The open circles indicate experimental values from either Chondros & Dimarogonas (1998) or Chondros (2001). It is clear that the computed values agree very well with the analytical ones; however, the two differ somewhat from the experimental values. This may be due to an inaccurate mathematical model or to unrefined experimental measurements. Nevertheless, the experimental program aimed at validating the lumped flexibility conducted first in Gudmunson (1983) on cracked cantilever beams validates the mathematical model and suggests that the discrepancies are due to experimental errors. A possible source of errors is the realization of the hinges for the vibration testing of the simply supported beam. Indeed, from the experimental viewpoint, the realization of hinges represents a much more challenging problem than fixing the edges. Furthermore, while the quoted experimental tests of Gudmunson (1983) were conducted on beams cracked by saw-cuts, those of Chondros & Dimarogonas (1998) and Chondros (2001) refer to fatigue cracks. It is well known that the controlled introduction of fatigue cracks involves several experimental difficulties not encountered in the saw cut method.

5.3 Transient analysis for a breathing crack

Here, we analyze free vibrations of the cracked beam when the crack is assumed to breath. We assume that the crack is located on the lower surface of the beam, the beam is initially undeformed and is excited according to the first mechanical mode shape of the intact beam. The

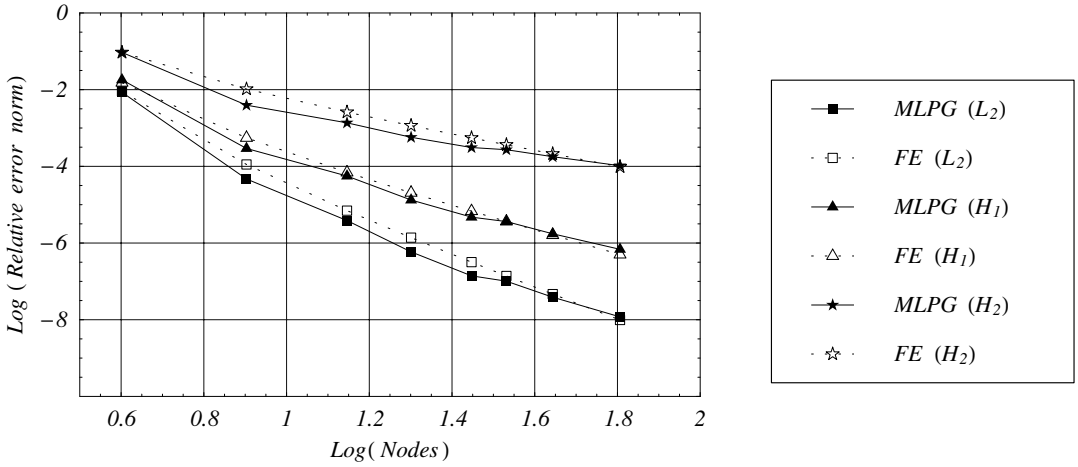

Figure 3 : For a uniformly loaded beam, convergence of the error norms with a decrease in the nodal spacing or an increase in the number of uniformly distributed nodes.

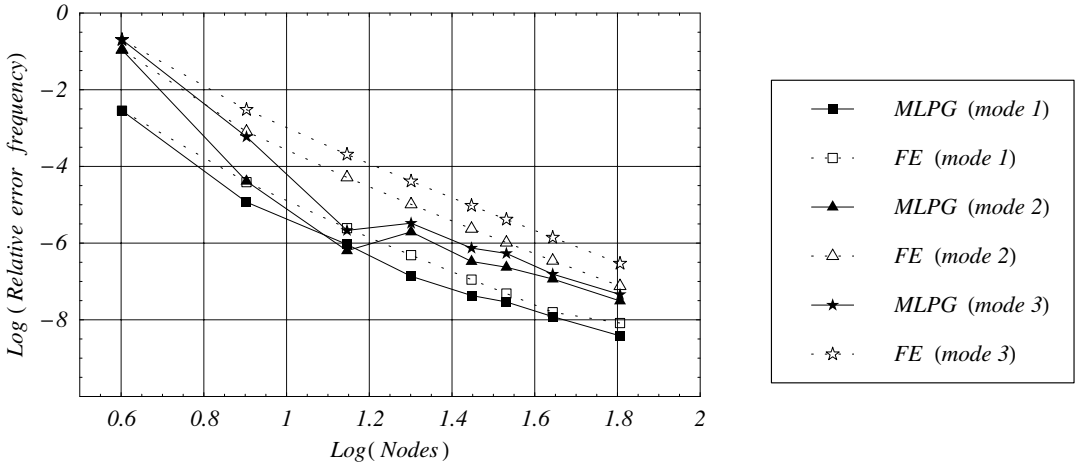

Figure 4 : Convergence rates of the first three natural frequencies.

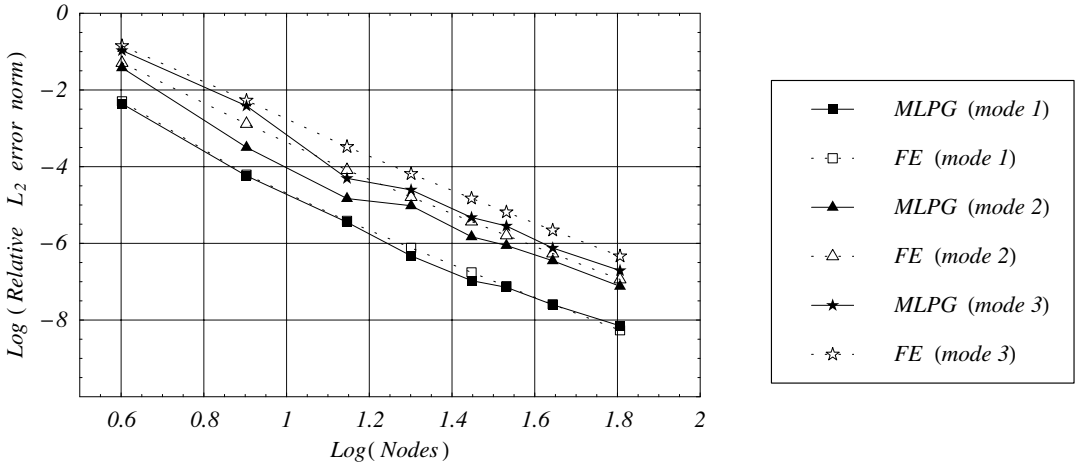

Figure 5 : Convergence rates of the three lowest modes in L_2 norm.

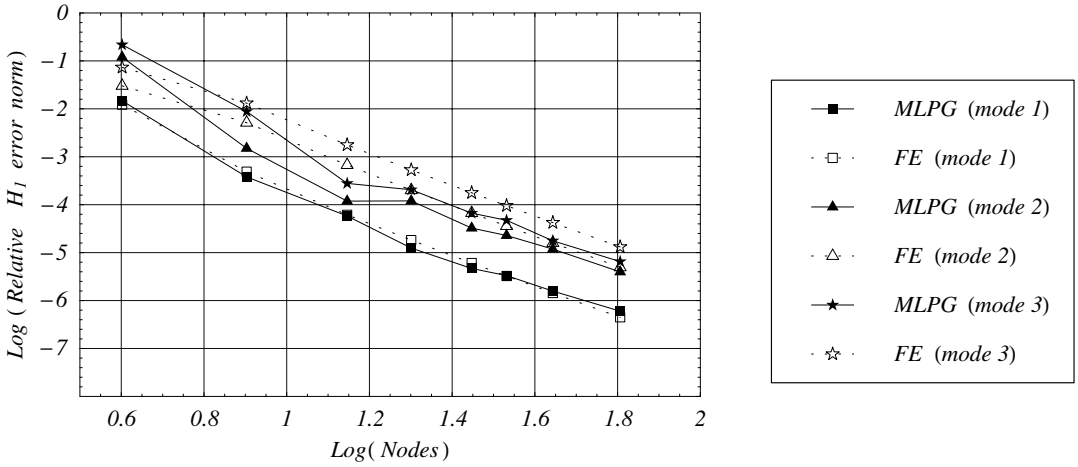

Figure 6 : Convergence rates of the three lowest modes in H_1 norm.

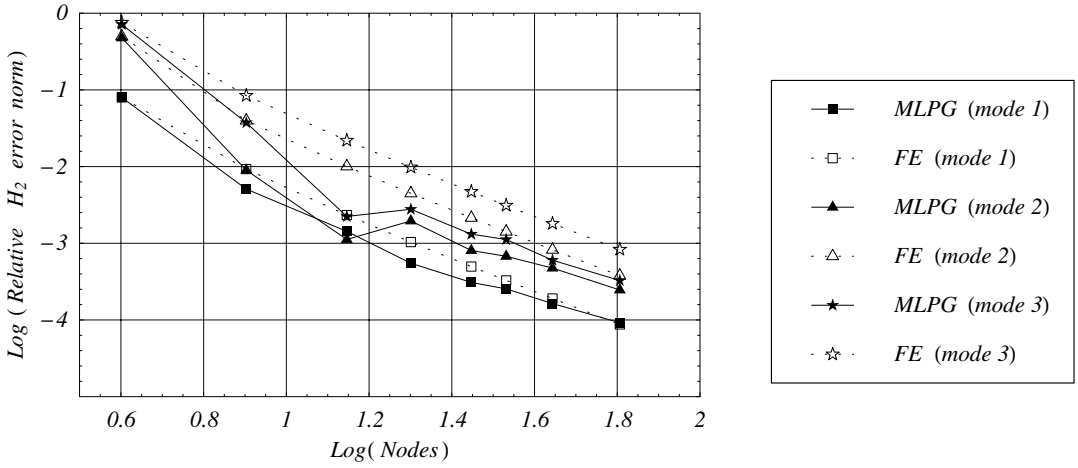

Figure 7 : Convergence rates of the three lowest modes in H_2 norm.

nonlinearity introduced by the bilinear behavior of the breathing crack does not allow for a simple analytical solution of the transient problem.

Accordingly, we compare our results with those obtained by the algorithm of Sundermeyer & Weaver (1995). The technique in Sundermeyer & Weaver (1995) relies on the *a priori* knowledge of the mode shapes of the intact beam and of the beam with the open crack and consists of consecutive calculations of the beam mode amplitudes. At each vibration cycle the deflection is expressed in terms of a finite number of mode shapes: if the crack is closed the modal shapes of the intact beam are used, otherwise the mode shapes of the cracked beam in (27) and (28) are used. The transition times between the two crack states are determined by continuously monitoring the sign of the curvature at the crack location. The initial conditions for free oscillations at each vibration cycle are determined by simply converting the sets of natural coordinates at the transition times. We note that at the instants of crack opening and closing, several concomitant mode shapes may arise since the mode shapes of the intact and the cracked beam are in general not orthogonal.

The numerical integration of governing equations (25) is performed by using the $4+4$ nodes configurations described in the previous subsection with $s=3$ and the damped unconditionally stable Newmark integration scheme (see e.g. Hughes (1987)) with

$$\beta = 0.3025, \quad \gamma = 0.6, \quad \Delta t = 1.04\,\mu s.$$

This choice of parameters introduces a small numerical damping, which rapidly damps out undesired oscillations at the transition instants. The transition times are com-

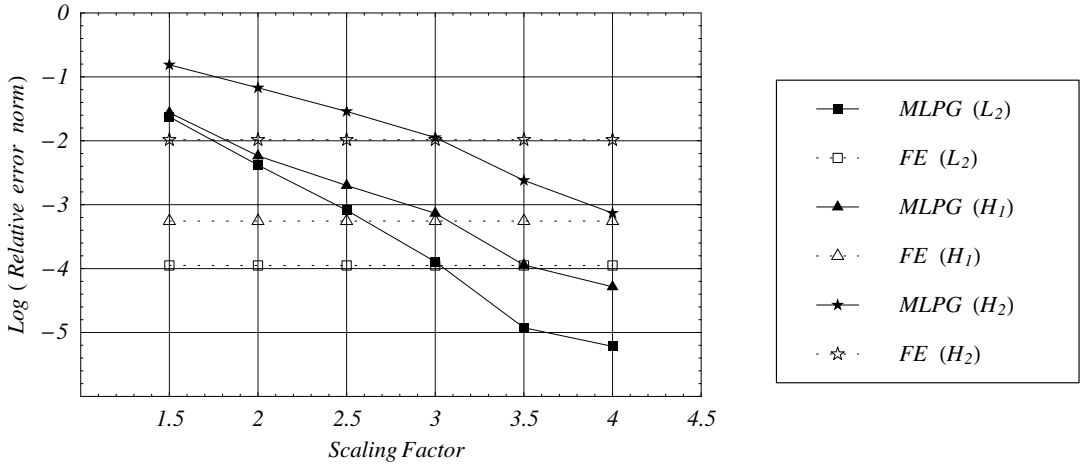

Figure 8 : For uniform loading and for $4+4$ nodes, relative error norms convergence with the weight functions radii.

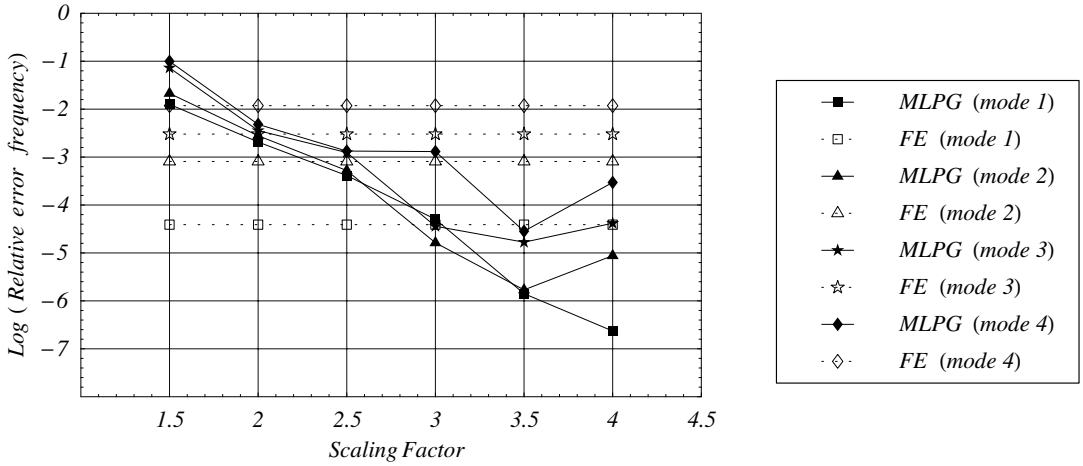

Figure 9 : Dependence of the relative error of the four lowest resonance frequencies for $4+4$ nodes upon the weight functions radii.

puted by continuously monitoring the average curvature at the crack location: i.e. the average between the curvatures of the two beam segments at the crack location.

In Figure 11 we compare the time evolutions of the deflection at the crack station computed with the proposed technique and that presented in Sundermeyer & Weaver (1995) with 25 mode shapes. Figure 12 compares the time history of the relative rotation at the crack station computed with the two methods. It is evident that the solution with the MLPG method agrees very well with that given in Sundermeyer & Weaver (1995).

5.4 Remarks

As is rather well known, Euler's beam theory simulates well deformations of a thin beam. For a thick beam one should employ either the Timoshenko beam theory or a higher-order shear and normal deformable beam theory such as that proposed by Batra & Vidoli (2002). Qian, Batra & Chen (2003a), Qian, Batra & Chen (2003b), Qian, Batra & Chen (2004a), Qian, Batra & Chen (2004b), Qian & Batra (2004) and Qian & Batra (2005) have studied by the MLPG method static and dynamic deformations of both homogeneous and functionally graded isotropic thick plates, and have compared the performance of the MLPG1 and the MLPG6 formulations. For a thick beam one will very likely need to

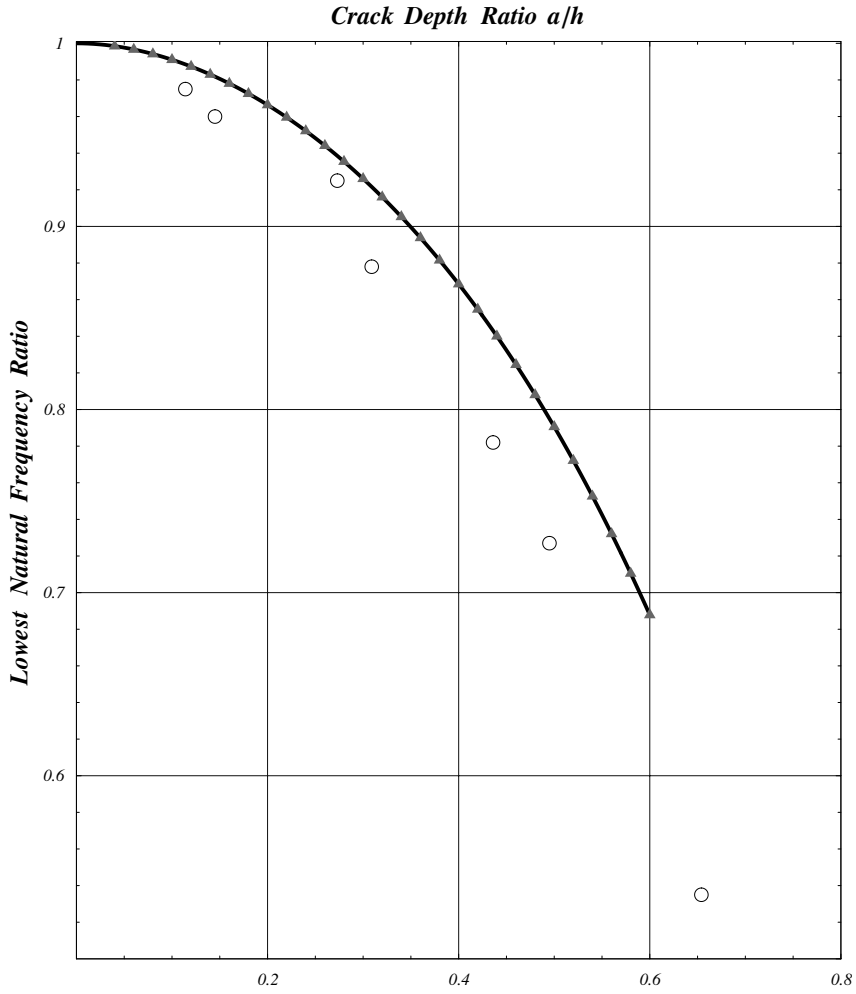

Figure 10 : Exact (solid), approximate (triangles) and experimental (circles) lowest frequency ratio with different crack severities.

modify the expression for the rotational spring constants k_i in equation (11).

We have considered cracks aligned along the depth of the beam which is appropriate for a thin beam. For cracks either parallel or inclined to the longitudinal centroidal axis of the beam, one will need to modify the problem formulation. Ching & Batra (2001), and Batra & Ching (2002) have applied the MLPG method to determine crack-tip fields in a pre-cracked plate deformed either statically or dynamically.

Even though the CPU time required to compute an element of the stiffness matrix in the MLPG6 formulation adopted here has been rather large as compared to that in the finite element method, Atluri, Han & Rajendran (2004) have shown that it is not so in their mixed MLPG formulation in which both displacements and strains are interpolated with the MLS basis functions. Furthermore, Atluri & Shen (2005) have demonstrated that the Euler-Bernoulli beam equation can be solved by using the standard MLS approximation and various mixed volume MLPG methods which are computationally more efficient than the FEM.

6 Conclusions

We have used the MLPG method to study vibrations of a cracked beam. When studying dynamic problems for cracked beams the penalty method does not seem to be adequate since it leads to ill-conditioned problems. Therefore, the treatment of vibrations of cracked beams necessitates the use of Lagrange multipliers to account for the relative rotation at the crack locations and satisfy

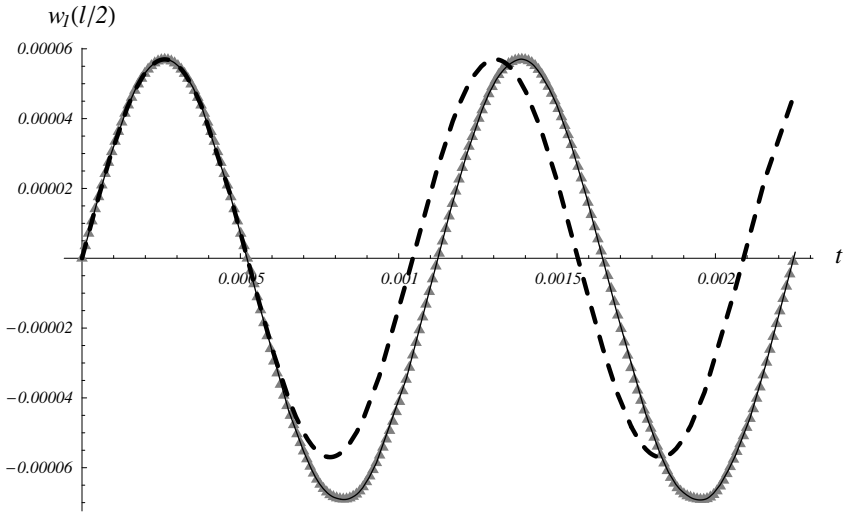

Figure 11 : Time evolution of the deflection field at the crack station: breathing crack with 25 mode shapes (solid), breathing crack with the MLPG method (triangles) and exact solution for the intact beam (dashed).

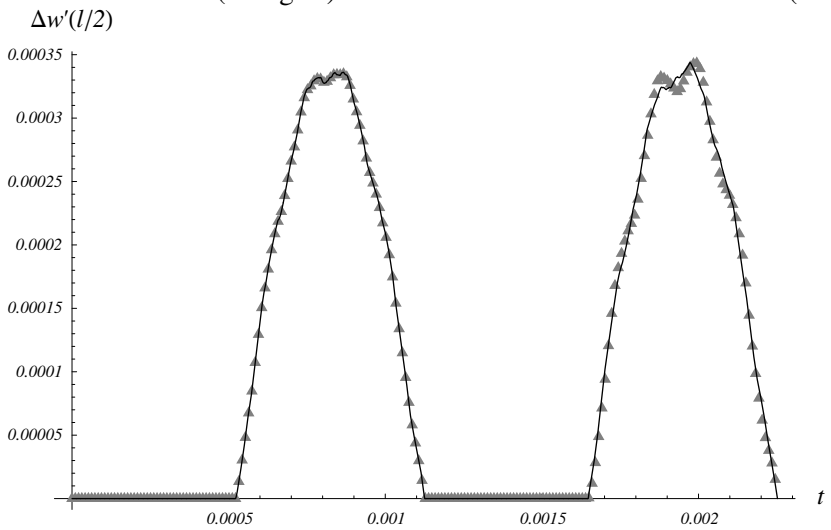

Figure 12 : Time evolution of the change of rotations at the crack station: breathing crack with 25 mode shapes (solid) and breathing crack with the proposed method (triangles).

the kinematic boundary conditions. The accurate estimation of the relative rotation at the crack locations is crucial for the identification process based on mode shapes (see e.g. Rizos, Aspragathos & Dimarogonas (1988)) and for the transient analysis of a breathing crack (see e.g. Sundermeyer & Weaver (1995)).

The stability of the method is assessed by analytically proving the inf-sup condition. The MLPG method is initially applied to compute the modal characteristics (both frequencies and mode shapes), and to analyze the transient and static deformations of beams with multiple open cracks. The derivation of reduced systems, where the imposed constraints are automatically satisfied, has been presented. It is also extended to treat the effects of breathing cracks on the dynamics of a cracked beam. Each crack is modeled as a bilinear spring with spring constant changing according to the value of the beam curvature at the crack location. Computational details for the derivation of the initial conditions at each vibration cycle have been provided. The numerical time integration is performed by the use of Newmark family of methods, and the spatial integration in the MLPG formulation employs Gaussian quadrature.

Numerical results for a simply supported beam are presented and compared with those obtained from analytical, finite element and semi-analytical methods. In par-

Table 1 : Comparison of the MLPG method and FEM for the vibrations of a cracked beam.

	MLPG	**FEM**
Weak formulation	Local	Global
Information needed about the nodes	Locations only	Locations and connectivity
Subdomains	Not necessarily disjoint	Disjoint
Trial functions	Relatively complex and difficult to express (GMLS) but easy to generate as closed-form expressions	Hermite polynomials
Integration rule	Higher order	Lower order
Mass matrix	Symmetric, banded, positive definite	Symmetric, banded, positive definite
Stiffness matrix	Symmetric, banded, positive semi-definite	Symmetric, banded, positive semi-definite
Assembly of equations	Required only for connecting different intact segments	Required
Stresses and strains	Smooth everywhere in the intact segments	Good at integration points
Addition of nodes	Easy	Difficult
Determination of time step size for stability in transient analysis	Relatively easy	Relatively easy
Imposition of essential boundary conditions	Lagrange multipliers are needed	Simple rows, columns deletions are needed
CPU time for computing a single matrix entry	Considerable	Little
Number of nodes required for high accuracy	Few	High
CPU time for a prescribed accuracy on the modal properties or on the static deformations	Moderate	Moderate

ticular, results of the MLPG method are compared with those of the FEM for both the static and the beam modal analysis. The convergence rates of the MLPG formulation are similar to those of the FEM, but for a fixed number of degrees of freedom the MLPG results are generally more accurate than the FE ones. Furthermore, the accuracy of the MLPG method may be controlled by modifying the supports of the weight function used in the GMLS approximation. It is shown that with few nodes and very large supports extremely accurate estimates of both the static deformations and the modal properties may be achieved. This represents a very favorable feature of the MLPG method with respect to the FEM. When comparing the computational time of the MLPG method with the computational time of the FEM for a fixed number of nodes the FEM clearly wins but, when the accuracy is also considered the comparison is not so bad. Indeed, very few nodes in the MLPG method may be satisfactory for highly accurate numerical solutions valid over wide frequency ranges. The possibility of using a reduced number of degrees of freedom is desirable when analyzing transient deformations with breathing cracks. Indeed, the use of small stiffness and mass matrices greatly alleviates the computational time when solving these non-

linear transient problems. The MLPG predictions are in very good agreement with those of the method of Sundermeyer & Weaver (1995), which is based on the knowledge of the exact cracked beam mode shapes and is difficult to extend to more complicated structures, such as cracked frames. Furthermore, the possibility of retaining reduced order numerical models may be crucial in identification or optimization processes when algorithms should be built based on the number of degrees of freedom.

The present implementation of MLPG method represents an interesting alternative to the classical FEM for the analysis of cracked beams (see Table 1 for a summary of comparison between the two methods).

Acknowledgement: The partial support of the Engineering Science and Mechanics Department of the Virginia Polytechnic Institute and State University is gratefully acknowledged by Maurizio Porfiri. This research has also been partially supported by the University of Rome "La Sapienza" Progetto di Ateneo 2004 "Soppressione delle vibrazioni mediante modifiche strutturali: modelli continui e discreti" (codice progetto C26A044385). The authors would like to thank Davide Spinello for the careful review of the manuscript. RCB was partially supported by the ONR grant N00014-98-1-0300 with Dr. Y.D.S. Rajapakse as the cognizant program manager.

References

Atluri, S. N.; Cho, J. Y.; Kim, H.-G. (1999): Analysis of thin beams, using the meshless local Petrov-Galerkin method, with generalized moving least squares interpolations. *Computational Mechanics,* vol. 24, pp. 334-347.

Atluri, S. N.; Han, Z. D.; Rajendran, A. M. (2004): A new implementation of the meshless finite volume method, through the MLPG "Mixed" approach. *CMES: Computer Modeling in Engineering & Sciences*, vol. 6, pp. 491-513.

Atluri, S. N.; Shen, S. (2002): The Meshless Local Petrov-Galrkin (MLPG) Method: A Simple & Less-costly Alternative to Finite Element and Boundary Element Methods. *CMES: Computer Modeling in Engineering & Sciences*, vol. 3, pp. 11-51.

Atluri, S. N.; Shen, S. (2005): Simulation of a 4th Order ODE: Illustration of Various Primal & Mixed MLPG Methods. *CMES: Computer Modeling in Engineering & Sciences*, vol. 7, pp. 241-268.

Atluri, S. N.; Zhu, T. (1998): A new Meshless Local Petrov-Galerkin (MLPG) approach in computational mechanics. *Computational Mechanics*, vol. 22, pp. 117-127.

Bathe, K. J. (1996): Finite Element Procedures. Prentice-Hall: Englewood Cliffs, New Jersey.

Batra, R. C.; Ching H.-K. (2002): Analysis of Elastodynamic Deformations near a Crack/Notch Tip by the Meshless Local Petrov-Galerkin (MLPG) Method. *CMES: Computer Modeling in Engineering & Sciences*, vol. 3, pp. 717-730.

Batra, R.; Porfiri, M; Spinello, D. (2004): Treatment of Material Discontinuity in Two Meshless Local Petrov-Galerkin (MLPG) Formulations of Axisymmetric Transient Heat Conduction. *International Journal of Numerical Methods in Engineering,* vol., 61, pp. 2461-2479.

Batra, R. C.; Vidoli, S. (2002): Higher Order Piezoelectric Plate Theory Derived from a Three-Dimensional Variational Principle. *AIAA Journal*, vol. 40, pp. 91-104.

Batra, R. C.; Wright, R. W. (1986): Steady State Penetration of Rigid Perfectly Plastic Targets. *Int. J. Engng Sci.*, Vol. 24, pp. 41-54.

Batra, R. C.; Zhang, G. M. (2004): Analysis of Adiabatic Shear Bands in Elasto-Thermo-Viscoplastic Materials by Modified Smoothed-Particle Hydrodynamics (MSPH) Method. *Journal of Computational Physics*, vol. 34, pp. 137-146.

Belytschko, T.; Lu Y.Y.; Gu, L. (1994): Element-free Galerkin methods. *International Journal of Numerical Methods in Engineering* vol. 37, pp. 229-256.

Carneiro, S. H. S.; Inman, D. J. (2002): Continuous model for the transverse vibration of cracked Timoshenko beams, *Transactions of the ASME* vol. 124, pp. 310-320.

Ching H.-K.; Batra, R. C. (2001): Determination of Crack Tip Fields in Linear Elastostatics by the Meshless Local Petrov-Galerkin (MLPG) Method. *CMES: Computer Modeling in Engineering & Sciences*, vol. 2, pp. 273-289.

Chondros, T. G.; Dimarogonas, A. D. (1998): A continuous cracked beam vibration theory. *Journal of Sound and Vibration*, vol. 215, pp. 17-34.

Chondros, T. G.; Dimarogonas, A. D. (2001): Vibration of a beam with a breathing crack. *Journal of Sound and Vibration*, vol. 239, pp. 57-67.

Chondros, T. G. (2001): The continuous crack flexibility model for crack identification. *Fatigue & Fracture of Engineering Materials & Structures*, vol. 24, pp. 643-650.

Christides, S.; Barr, A. D. S. (1984): One-dimensional theory of cracked Bernoulli-Euler beams. *International Journal of Mechanical Sciences,* vol. 26, pp. 639-648.

Dimarogonas, A. D. (1996): Vibration of cracked structures: A state of the art review. *Engineering Fracture Mechanics*, vol. 55, pp. 831-857.

Duarte, C. A. M.; Oden, J. T. (1996): Hp clouds—an hp meshless method. *Numerical Methods for Partial Differential Equations*, vol. 12, pp. 673–705.

Ferreira, A. J. M.; Batra, R. C.; Roque, C. M. C.; Qian L. F. and Martins, P. A. L. S. (2005). Static Analysis of Functionally Graded Plates Using Third-order Shear Deformation Theory and a Meshless Method. *Composite Structures*, vol. 69, pp. 449-457.

Gounaris, G.; Dimarogonas, A. (1998): A finite element of a cracked prismatic beam for structural analysis. *Computers & Structures*, vol. 28, pp. 309-313.

Gounaris, G.; Papadoupolos C. A.; Dimarogonas, A. (1996): Crack Identification in beams by coupled response measurements. *Computers & Structures,* vol. 58, pp. 299-305.

Gudmunson, P. (1983): The dynamic behaviour of slender structures with cross-sectional cracks. *Journal of the Mechanics and Physics of Solids*, vol. 31, pp. 329-345.

Hughes, T. J. R. (1987): The finite element method. Linear static and dynamic finite element Analysis. Prentice-Hall: New Jersey.

Kansa, E.J. (1990): Multiquadrics- a Scattered Data Approximation Scheme with Application to Computational Fluid Dynamics. ii: Solutions to Parabolic, Hyperbolic and Elliptic Partial Differential Equations. *Computer & Mathematics with Applications*, vol. 19, pp. 147-161.

Khiem, N. T.; Lien T. V. (2004): Multi-crack detection for beam by the natural frequencies. *Journal of Sound and Vibration*, vol. 273, pp. 175-184

Lancaster, P.; Salkauskas, K. (1981): Surfaces generated by moving least squares methods. *Mathematics of Computation,* vol. 37, pp. 141-158.

Liu, W.; Jun, S; Zhang, Y. (1995): Reproducing kernel particle method. *International Journal for Numerical Methods in Fluids*, vol. 20, pp. 1081-1106.

Lucy, L. B. (1977): A numerical approach to the testing of the fission hypothesis. *The Astronomical Journal*, vol. 82, pp. 1013-1024.

Luzzato, E. (2003): Approximate computation of nonlinear effects in a vibrating cracked beam. *Journal of Sound and Vibration*, vol. 265, pp. 745-763.

Mahmoud, M. A.; Zaid, M. A.; Al Harashani, S. (1999): Numerical frequency analysis on uniform beams with a transverse crack. *Communications in Numerical Methods in Engineering*, vol. 15, pp. 709-715.

Melenk, J. M.; Babuska, I. (1996): The partition of unity finite element method: Basic theory and applications, *Computer Methods in Applied Mechanics and Engineering*, vol. 139, pp. 289-314.

Nayroles, B.; Touzot, G.; Villon, P. (1992): Generalizing the finite element method: diffuse approximation and diffuse elements. *Computational Mechanics*, vol. 10, pp. 307-318.

Ostachowicz, W. M.; Krawczuk, M. (1991): Analysis of the effect of cracks on the natural frequencies of a cantilever beam. *Journal of Sound and Vibration*, vol. 150, pp. 191-201.

Pugno, N.; Surace, C.; Ruotolo, R. (2000): Evaluation of the non-linear dynamic response to harmonic excitation of a beam with several breathing cracks. *Journal of Sound and Vibration*, vol. 235, pp. 749-762.

Qian, L. F.; Batra, R. C. (2004): Transient Thermoelastic Deformations of a Thick Functionally Graded Plate. *Journal of Thermal Stresses*, vol. 27, pp. 705-740.

Qian, L. F.; Batra, R. C. (2005): Design of Bidirectional Functionally Graded Plate for Optimal Natural Frequencies. *Journal of Sound and Vibration*, vol. 280, pp. 415-424.

Qian, L. F.; Batra, R. C.; Chen, L. M. (2003a): Elastostatic Deformations of a Thick Plate by using a Higher-Order Shear and Normal Deformable Plate Theory and Two Meshless Local Petrov-Galerkin (MLPG) Methods. *CMES: Computer Modeling in Engineering & Sciences*, vol. 4, pp. 161-176.

Qian, L. F.; Batra, R. C.; Chen, L. M. (2003b): Free and Forced Vibrations of Thick Rectangular Plates by using Higher-Order Shear and Normal Deformable Plate Theory and Meshless Petrov-Galerkin (MLPG) Method. *CMES: Computer Modeling in Engineering & Sciences*, vol. 4, pp. 519-534.

Qian, L. F.; Batra, R. C.; Chen, L. M. (2004a): Static and Dynamic Deformations of Thick Functionally Graded Elastic Plate by using Higher-Order Shear and Normal Deformable Plate Theory and Meshless Local Petrov-Galerkin Method. *Composites: Part B*, vol. 35, pp. 685-697.

Qian, L. F.; Batra, R. C.; Chen, L. M. (2004b): Analysis of Cylindrical Bending Thermoelastic Deformations of Functionally Graded Plates by a Meshless Local Petrov-Galerkin Method. *Computational Mechanics*, vol. 33, pp. 263-273.

Qian, G. L.; Gu, S.-N.; Jiang, J.-S. (1990): The dynamic behaviour and crack detection of a beam with a crack. *Journal of Sound and Vibration*, vol. 138, pp. 233-243.

Raju, I. S, Phillips, D. R. (2003): Further developments in the MLPG Method for Beam Problems. *CMES: Computer Modeling in Engineering & Sciences,* vol. 4, pp. 141-159.

Rizos, P. F.; Aspragathos, N.; Dimarogonas, A. D. (1988): Identification of crack location and magnitude in a cantilever beam from the vibration mode. *Journal of Sound and Vibration*, vol. 138, pp. 381-388.

Ruotolo, R.; Surace, C.; Crespo, P.; Storer, D. (1996): Harmonic analysis of the vibrations of a cantilevered beam with a closing crack. *Computers & Structures*, vol. 61, pp. 1057-1074.

Shen, M.-H. H.; Chu, Y. C. (1992): Vibrations of a beam with a fatigue crack. *Computers & Structures*, vol. 45, pp. 79-93.

Shen, M.-H. H; Pierre C. (1990): Natural modes of Bernoulli-Euler beams with symmetric cracks. *Journal of Sound and Vibration*, vol. 138, pp. 115-134.

Shen, M.-H. H; Pierre, C. (1994): Free vibrations of beams with single-edge crack. *Journal of Sound and Vibration*, vol. 170, pp. 237-259.

Sukumar, N.; Moran, B.; Belytschko, T. (1998): The natural element method in solid mechanics. *International Journal for Numerical Methods in Engineering*, vol. 43, pp. 839-887.

Sundermeyer, J. M.; Weaver, R. L. (1995): On crack identification and characterization in a beam by nonlinear vibration analysis. *Journal of Sound and Vibration*, vol. 183, pp. 857-871.

Warlock, A.; Ching, H.-K.; Kapila A. K.; Batra, R. C. (2002): Plane Strain Deformations of an Elastic Material Compressed in a Rough Rectangular Cavity. *International Journal of Engineering Science*, vol. 40, pp. 991-1010.

Wendland, H. (1995): Piecewise polynomial, positive definite and compactly supported radial basis functions of minimal degree. *Advances in Computational Mathematics,* vol. 4, pp. 389-396.

Zhang G. M.; Batra R. C. (2004): Modified smoothed particle hydrodynamics method and its application to transient problems. *Computational Mechanics*, vol. 34, pp. 137-146.